Structural and magnetoelectric properties of $Ga_{2-x}Fe_xO_3$ single crystals grown by a floating-zone method

T. Arima,[1,2,*] D. Higashiyama,[3] Y. Kaneko,[1] J. P. He,[1] T. Goto,[3] S. Miyasaka,[3] T. Kimura,[3,†] K. Oikawa,[4] T. Kamiyama,[4] R. Kumai,[5] and Y. Tokura[1,3,5]

[1]*Spin Superstructure Project, ERATO, Japan Science and Technology Agency, AIST Tsukuba Central 4, Tsukuba 305-8562, Japan*

[2]*Institute of Materials Science, University of Tsukuba, Tsukuba 305-8573, Japan*

[3]*Department of Applied Physics, University of Tokyo, Tokyo 113-8656, Japan*

[4]*Neutron Science Laboratory, Institute of Materials Structure Science, High Energy Accelerator Research Organization, Tsukuba 305-0801, Japan*

[5]*Correlated Electron Research Center (CERC), National Institute of Advanced Industrial Science and Technology (AIST), Tsukuba 305-8562, Japan*

(Received 8 December 2003; revised manuscript received 5 April 2004; published 31 August 2004)

Lattice-structural, magnetic, and magnetoelectric (ME) properties have been investigated for single crystals of prototypical polar ferrimagnet $Ga_{2-x}Fe_xO_3$ ($0.8 \leqslant x \leqslant 1.4$) as melt-grown by a floating-zone (FZ) method. Magnetization measurements show that the saturated magnetization as well as the ferrimagnetic phase transition temperature (T_C) increases with as increase of Fe content x, while the coercive force decreases. A neutron powder diffraction study indicates fairly low ordering of Ga and Fe arrangement at cation sites, which is likely related to the lower T_C in the FZ crystals than in the corresponding flux-grown crystals. Coefficients of linear and quadratic ME effects have been obtained with measurements of change in electric polarization induced by sweeping a magnetic field. Electric polarization was largely modulated in a magnetic field applied parallel to the direction of spontaneous magnetization, but not in a field parallel to that of the spontaneous polarization. A simple model to explain the sharp contrast is presented.

DOI: 10.1103/PhysRevB.70.064426 PACS number(s): 75.50.Gg, 75.80.+q, 61.12.Ld, 75.25.+z

I. INTRODUCTION

$Ga_{2-x}Fe_xO_3$ ($0.5 \leqslant x \leqslant 1.6$), which was synthesized by Remeika, is piezoelectric and also shows spontaneous magnetization at low temperatures.[1] It has an orthorhombic unit cell with $a \sim 8.8$ Å, $b \sim 9.4$ Å, and $c \sim 5.1$ Å.[2] The crystal structure is shown in Fig. 1(a).[3–5] The space group is $Pc2_1n$, which indicates the spontaneous polarization along the b axis.[6] In the low-temperature phase, the spin moments of Fe1 and Fe2 are directed nearly to $\pm c$ and antiferromagnetically coupled.[5,7] The compound behaves as a ferrimagnet since the Fe occupations at the Fe1 and Fe2 sites are slightly different from each other.

Such a polar magnet shows magnetoelectric (ME) effects. By applying a magnetic field $\boldsymbol{H}$, electric polarization $\boldsymbol{P}$ can be modulated (ME_H effect). ME tensors $\boldsymbol{\alpha}$ and $\boldsymbol{\beta}$ are defined in SI units as[8]

$$\Delta P_i = \sum_j \alpha_{ij} H_j + \frac{1}{2} \sum_{j,k} \beta_{ijk} H_j H_k + O(H^3).$$

Conversely, magnetization $\boldsymbol{M}$ can be induced by applying an electric field $\boldsymbol{E}$ (ME_E effect) as

$$\mu_0 \Delta M_j = \sum_i \alpha_{ij} E_i + O(E^2).$$

Since the magnetic easy axis is c in $Ga_{2-x}Fe_xO_3$, it belongs to $m'2'm$ in the Schubnikov group. In terms of the group theory, one can expect two nonzero elements in the $\boldsymbol{\alpha}$ tensor, α_{bc} and α_{cb}. A large linear ME effect in $Ga_{2-x}Fe_xO_3$ was reported by Rado,[9] $\alpha_{bc} \approx 3 \times 10^{-4}$ (cgs-gauss unit) $\approx 1 \times 10^{-11}$ (s/m) (SI unit) at 77 K in a flux-grown $x \approx 1$ crystal.

It has been pointed out that magnetoelectrics can also show some optical/x-ray phenomena, termed gyrotropic magneto-optics, magnetochiral effect, and magnetic second-harmonic generation.[10–15] In order to study the magneto-optics, one needs to prepare a large single-domain crystal. Single crystals grown from Bi_2O_3-B_2O_3 flux, which were previously used for the study of ME effects, do not have an enough dimension along the polar b axis. In this paper, we report the successful crystal growth of $Ga_{2-x}Fe_xO_3$ by a floating-zone (FZ) method. Single crystalline rods with a diameter of ≈ 5 mm and a length of several centimeters could be prepared. We found that the preparation method influenced the magnetic transition temperature. Neutron diffraction measurements revealed that the difference in T_C is likely caused by the change in the Ga/Fe occupations at the four types of cation sites. A coefficient of a linear ME effect α_{bc} is nearly equal to the value previously reported for flux-grown crystals.[9,16] We also tried to measure another linear ME coefficient α_{cb}, but the electric polarization along the c axis induced by a magnetic field along the b axis is too small ($|\alpha_{cb}| < 1 \times 10^{-12}$ s/m) to be detected. A quadratic behavior of the polarization along the b axis as a function of magnetic field along the a or b axis is also presented.

II. CRYSTAL GROWTH AND CHARACTERIZATION

Crystals of $Ga_{2-x}Fe_xO_3$ with $0.8 \leqslant x \leqslant 1.4$ were successfully grown by a FZ method. Powders of Ga_2O_3 and Fe_2O_3 with purities of 99.9% were weighed to the prescribed ratios, mixed, and well ground. The mixture was heated at 1350 °C for 10 h in air and then pulverized. We confirmed by powder

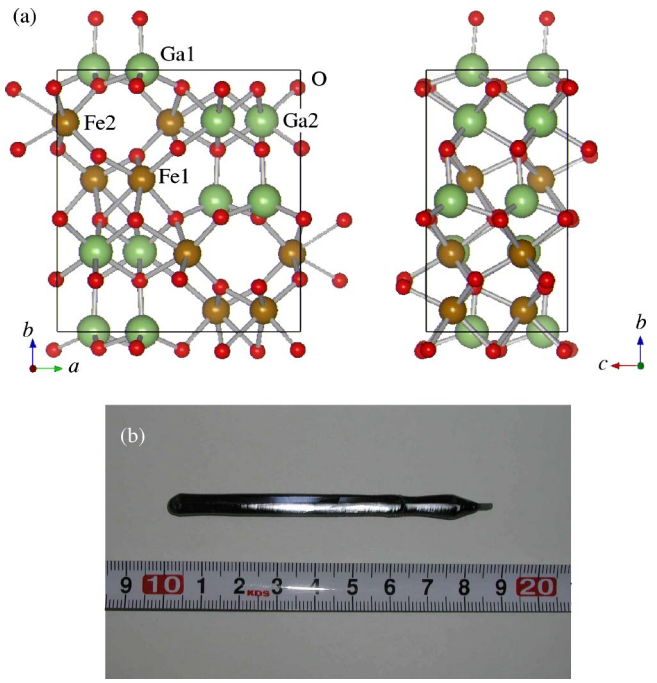

FIG. 1. (Color online) (a) Crystal structure of $Ga_{2-x}Fe_xO_3$. Projection views along the (left) *c* and (right) *a* axes. (b) A melt-grown single crystalline boule of $Ga_{2-x}Fe_xO_3$ with $x=1.0$.

x-ray diffraction (XRD) measurements that the obtained powders were of single phase of the orthorhombic $Ga_{2-x}Fe_xO_3$. The resulting powders were pressed into a rod with a diameter of ~5 mm and a length of ~10 cm and sintered again at 1350 °C for 30 h in air. According to the phase diagram of the Ga_2O_3-Fe_2O_3 system,[17] the orthorhombic $GaFeO_3$ melts incongruently at ~1520 °C in air. However, the phase diagram under 10 atm O_2 indicates that $Ga_{2-x}Fe_xO_3$ can be obtained from the melt. We therefore performed the crystal growth under 9–10 atm oxygen gas, using a halogen-lamp image furnace (NEC machinery, SC-M35HD) at a rate of 2–3 mm/h. We show in Fig. 1(b) a photograph of a grown crystal boule with $x=1.0$. Obtained crystals were characterized by both powder and single-crystal XRD measurements. All the peaks can be indexed by the $Pc2_1n$ orthorhombic unit cell of $Ga_{2-x}Fe_xO_3$. For some samples, the Fe content was measured by inductively coupled plasma emission spectroscopy (ICP). The discrepancy of *x* between the prescribed and actual contents was within 0.01. The systematic change of the lattice constants and magnetic properties also ensures good control over *x*. Laue photographs indicated that the grown boule with $0.8 \leqslant x \leqslant 1.1$ was a single crystal free from twins. No domain boundaries were observed with a polarizing microscope for the *x* range.

III. MAGNETIC PROPERTIES

Magnetization of $Ga_{2-x}Fe_xO_3$ single crystals was measured by using a commercial superconducting quantum interference device magnetometer (Quantum Design, MPMS-5S). The observed magnetic properties agree with those reported

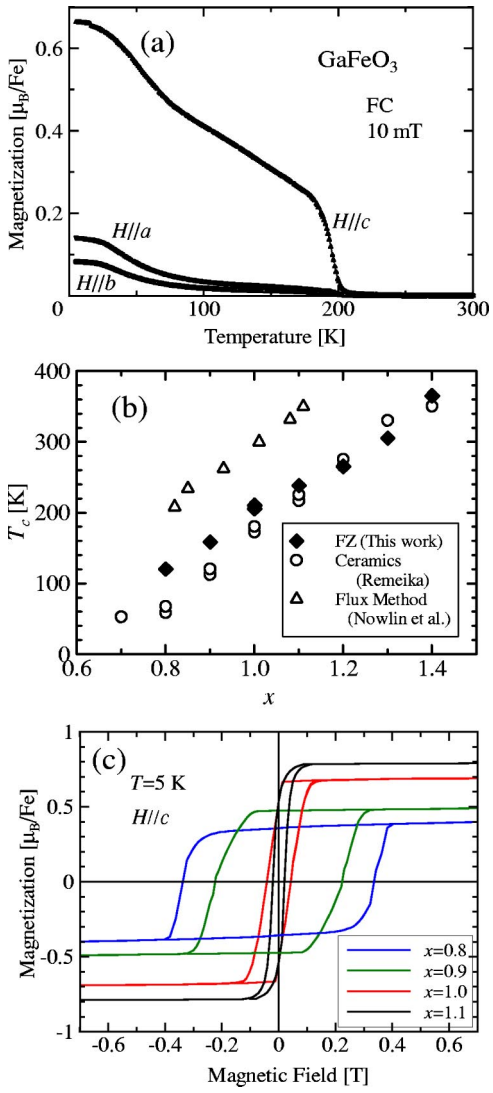

FIG. 2. (Color online) (a) Temperature dependence of magnetization of $Ga_{2-x}Fe_xO_3$ with $x=1.0$ in field-cooling (FC) runs for three different directions of an applied magnetic field (10 mT). (b) Magnetic transition temperature T_C in $Ga_{2-x}Fe_xO_3$ as a function of *x*. The value of T_C is also remarkably dependent on the method of sample preparation. Solid triangles: single crystals grown by a floating-zone method (this work). Open triangles: single crystals grown from Bi_2O_3-B_2O_3-flux (Ref. 1). Open circles: ceramics samples (Ref. 18). (c) Magnetization curves of $Ga_{2-x}Fe_xO_3$ with $x=0.8, 0.9, 1.0$, and 1.1 at 5 K. A magnetic field was applied along the *c* axis (easy axis).

by previous studies[4,18–20] as a whole, except for the ferromagnetic temperature. Spontaneous magnetization is observed in all the samples. The magnetization along the *c* axis of the $x=1.0$ sample in a 10 mT magnetic field shows a steep rise at about 200 K as shown in Fig. 2(a), which manifests the homogeneity of the sample. The relatively small magnetization at the lowest temperature is ascribed to ferrimagnetic ordering as discussed later. The magnetic easy axis is *c*. We define a cusp position in a field-cooling magnetization curve in 10 mT as the ferrimagnetic phase transition temperature (T_C). The possible shift of T_C caused by the external magnetic field is estimated to be less than 5 K from the compari-

son among the magnetization curves in various magnetic fields, which is small enough for investigation of the systematic change in T_C with the iron content x and preparation method.

The T_C value becomes higher as the iron content x increases as shown in Fig. 2(b). The comparison of T_C data with previous reports clearly indicates that T_C depends not only on x but also on how the compound was prepared. Single crystals grown from Bi_2O_3-B_2O_3 flux have higher T_C than single crystals grown by a FZ method and ceramics synthesized by solid state reaction. What is structurally and hence magnetically important is that in $Ga_{2-x}Fe_xO_3$ compounds the Fe sites are partially occupied with Ga and vice versa.[3–5] The random occupation of cations would be suppressed in the compounds synthesized with a lower temperature process. The difference in T_C between the flux- and FZ-grown crystals is possibly due to the different Ga/Fe occupations at cation sites between them. In the case of the Bi_2O_3-B_2O_3 flux method, the mixture of Ga_2O_3 and Fe_2O_3 is soaked in the flux at 1100 °C and slowly cooled down to 800 °C,[1,2] which is much lower than in the case of the FZ-melt single crystals (melting point ≈1600 °C) and the ceramics samples sintered at 1200–1400 °C. In addition, annealing of a flux-grown crystal at 1300 °C in air decreased the Curie temperature, which also confirms our speculation that the preparation temperature of the gallium ferrite considerably affects the magnetic properties. The Ga/Fe distribution in the crystals grown from flux at low temperatures is more ordered than the compounds with the same composition prepared by other methods such as a FZ method.

There might be other possible reasons which would cause the difference in T_C. For example, it is often observed in some ferrites that some kind of deficiencies would also affect the T_C value. As for the cation deficiency, we could not find any evidence in the neutron diffraction and ICP data. There is very little oxygen deficiency in the FZ crystals because the T_C was not altered at all upon annealing the FZ crystals at 1100 °C. To settle the issue, however, further detail comparison of various characterizations among the samples with various methods is necessary.

Magnetization curves along the easy axis c at 5 K are shown for various Fe content x in Fig. 2(c). The saturated ferrimagnetic magnetization increases from 0.4 μ_B per Fe ion for $x=0.8$ to 0.8 μ_B per Fe ion for $x=1.1$. Ferrimagnetic magnetization mainly originates from the difference in Fe occupation at the four inequivalent cation sites. The change in magnetization indicates that the rate of the increase in Fe content is different among the cation sites. Large x dependence is also observed in coercive force of $Ga_{2-x}Fe_xO_3$. The $x=0.8$ compound is a relatively hard magnet with the coercive force at 5 K larger than 0.3 T. The compound becomes a softer magnet with the increase of x, in spite of the increasing magnetization. The coercive force in the $x=1.1$ compound is an order of magnitude smaller than that in the $x=0.8$ compound. The x-dependent coercive force affects the magnetic-field-induced polarization as mentioned below.

IV. NEUTRON DIFFRACTION

Powder neutron diffraction pattern was measured using a time-of-flight (TOF) diffractometer Vega, KEK, Japan. FZ-grown single crystals with various compositions were pulverized for this purpose. High-resolution TOF data collected with a backward bank are analyzed by using a Rietveld program RIETAN-2001T.[21] The typical resolution is 0.25%. The obtained patterns and the fitting curves at 230 and 4 K are shown in Figs. 3(a) and 3(b). The structural parameters of the $x=1.0$ compound ($GaFeO_3$) at 230 K ($T>T_C$) are listed in Table I. All the coordinates agree well with the previous result[3–5] for the single crystal grown from the flux. Fe1 and Fe2 ions are located in distorted oxygen-octahedra and the displacements from the center of the octahedron along the b axis are +0.26 and −0.11 Å, respectively. The simple point-

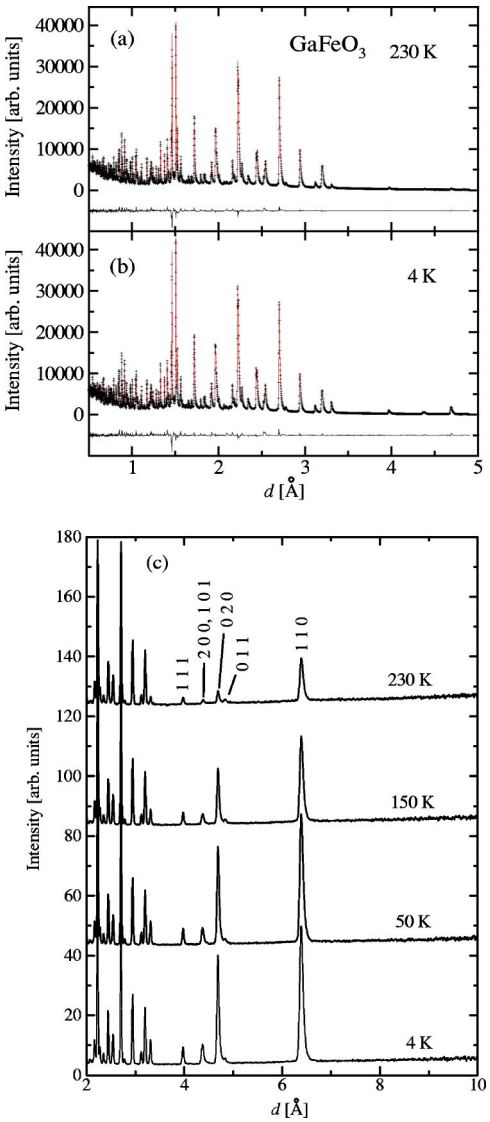

FIG. 3. (Color online) Time-of-flight neutron diffraction patterns in $GaFeO_3$. (a), (b) High-resolution data at 230 and 4 K collected by using a backward scattering bank. These data are fitted by using a Rietveld method. The difference of the data and fitting curves are shown by solid lines in the lower part of the respective panels. Fitting parameters are listed in Table I. (c) Wide-d-range data at various temperatures collected by using a 30° scattering bank to investigate magnetic scattering which appears in the large d range. A magnetization measurement of this sample showed that $T_C \approx 205$ K.

TABLE I. Structural parameters of $GaFeO_3$ at 230 and 4 K obtained by Rietveld analyses of time-of-fight neutron diffraction patterns using RIETAN-2001T (Ref. 21). The space group is $Pc2_1n$. The cell parameters are $a=8.725\,69(11)$ Å, $b=9.372\,09(13)$ Å, and $c=5.070\,82(7)$ Å at 230 K and $a=8.719\,32(13)$ Å, $b=9.368\,38(15)$ Å, and $c=5.067\,23(8)$ Å at 4 K. The y parameter of Ga1-fixed to zero. Isotropic thermal parameters (B) were used in the fitting. The occupation factors were obtained from the best fit of the 230-K pattern, and fixed in the analysis of the 4-K pattern. The Fe^{3+} magnetic moments an the Fe1, Fe2, and Ga2 sites at 4 K are −3.9, +4.5, and +4.7 μB/Fe, respectively. The Fe moment on the Ga1 site could not be determined because the Fe occupancy is too small. The reliabilty factors are as follows: $R_{wp}=0.0448$, $R_p=0.0331$ at 230 K, and $R_{wp}=0.0538$, $R_p=0.0375$ at 4 K.

	230 K				4 K			
	x	y	z	B	x	y	z	B
Ga1	0.1501(4)	0	0.1761(5)	0.18(4)	0.1500(4)	0	0.1781(6)	0.06(6)
Ga2	0.1597(3)	0.3067(4)	0.8091(5)	0.07(4)	0.1593(3)	0.3073(4)	0.8106(6)	0.01(6)
Fe1	0.1525(4)	0.5827(3)	0.1893(6)	0.12(4)	0.1538(4)	0.5831(3)	0.1886(6)	0.01(6)
Fe2	0.0351(2)	0.7992(4)	0.6787(5)	0.24(4)	0.0346(2)	0.7998(5)	0.6795(5)	0.04(10)
O1	0.3223(4)	0.4260(5)	0.9740(8)	0.44(7)	0.3228(5)	0.4262(5)	0.9716(9)	0.10(10)
O2	0.4877(4)	0.4313(6)	0.5168(7)	0.49(9)	0.4864(4)	0.4311(6)	0.5142(8)	0.10(10)
O3	0.9963(5)	0.2008(7)	0.6521(9)	0.20(6)	0.9979(6)	0.2022(5)	0.6541(10)	0.09(10)
O4	0.1593(5)	0.1961(4)	0.1475(8)	0.20(6)	0.1593(6)	0.1974(4)	0.1480(9)	0.05(9)
O5	0.1715(5)	0.6714(4)	0.8410(10)	0.25(6)	0.1695(5)	0.6717(5)	0.8437(10)	0.04(8)
O6	0.1725(4)	0.9379(5)	0.5153(9)	0.36(7)	0.1736(5)	0.9383(5)	0.5166(10)	0.11(9)

charge calculation indicates that the electrical polarization of $GaFeO_3$ along the b axis is as large as $-0.025\ C/m^2$, although the estimate is naive because the electron hybridization is totally neglected in the calculation.

Superexchange interaction between neighboring Fe^{3+} ions in the compound should be affected by the Fe-O-Fe bond angles. The larger bond angle generally results in the stronger antiferromagnetic superexchange. Calculating from the structural parameters listed in Table I, the Fe1-O1-Fe2 bond has the largest angle of 166° among all the cation-oxygen-cation bonds. Here we use the notation $M1$-O-$M2$ when the y coordinates of $M1$, O, and $M2$ satisfy the relation, $y(M1)>y(O)>y(M1)$. We can ascribe the ferrimagnetic ordering to the Fe1-O-Fe2 bond with such a large bond angle. The second largest value of 164° is observed in the Fe1-O1-Ga2 bond, which should result in the strong antiferromagnetic coupling between Fe1 and excess Fe at Ga2. In fact, the moment at Fe1 is aligned antiparallel to the Fe moment at Ga2 as mentioned later. The replacement of Ga with Fe at Ga2 should raise T_C through the strong antiferromagnetic coupling. In contrast, all the bond angles related to the Ga1 site are more deviated from 180°, 112°, 126°, 123°, and 114° for Fe2-O4-Ga1, Ga2-O4-Ga1, Ga1-O6-Fe2, and Ga1-O2-Ga2 bonds, respectively. The substitution of Fe at the Ga1 sites should less affect the T_C value than that at Ga2.

The Ga/Fe occupation parameters at the cation sites obtained from the best fit of the diffraction patterns at room temperature are listed in Table II. One can note that the Fe occupations at the Fe1, Fe2, and Ga2 sites for $x=1.15$ crystals are smaller than those reported by the previous reports on a corresponding flux-grown crystal.[4,5] The antiferromagnetic Fe-O-Fe network should weaken as the Ga amount at the Fe1, Fe2, and Ga2 sites increases. This is the most plausible reason for the lower T_C nature in the FZ-grown crystals than in the flux-grown crystals.

The ferrimagnetic ordering at low temperatures is proved by magnetic peaks in the neutron diffraction patterns as shown in Fig. 3(c). These patterns for a wide d-range were obtained at a 30° scattering bank. Some large-d Bragg peaks such as 110, 020, and 111 in the TOF patterns are found to grow below T_C, while no additional peaks are observed. The largely enhanced 020 peak suggests the antiferromagnetic arrangement of Fe1 and Fe2 spin moments in the ac plane. As demonstrated in Fig. 2(a), the easy and hard axes are c and b, respectively. The spontaneous magnetization along the c axis is caused either by a difference in magnetic moment on the Fe1 and Fe2 sites (ferrimagnetism) or by a small canting of the Fe moment (canted antiferromagnetism). The previous polarized neutron study[5] has evidenced the ferrimagnetic spin ordering. The magnetic contribution of all the large-d peaks in the present neutron diffraction pattern is also better fitted with the ferrimagnetic structure than with the

TABLE II. Fe partial occupancies at the Ga1, Ga2, Fe1, and Fe2 sites [see Figs. 1(a) and 1(b)] as deduced by a Rietveld analysis of time-of-flight neutron powder diffraction of FZ-melt samples at room temperature. The parameters for the flux-grown $x=1.15$ crystal reported in Refs. 4 and 5 are also listed for comparison.

x	Ga1	Ga2	Fe1	Fe2
0.80 (FZ)	0.08	0.18	0.73	0.62
0.90 (FZ)	0.12	0.35	0.74	0.59
1.00 (FZ)	0.18	0.35	0.77	0.70
1.10 (FZ)	0.11	0.46	0.79	0.84
1.15 (FZ)	0.17	0.49	0.81	0.83
1.15 (flux)[a]	≈0 (<0.04)	0.54	0.87	0.90
1.15 (flux)[b]	0.08	0.62	0.87	0.73

[a]Reference 4.
[b]Reference 5.

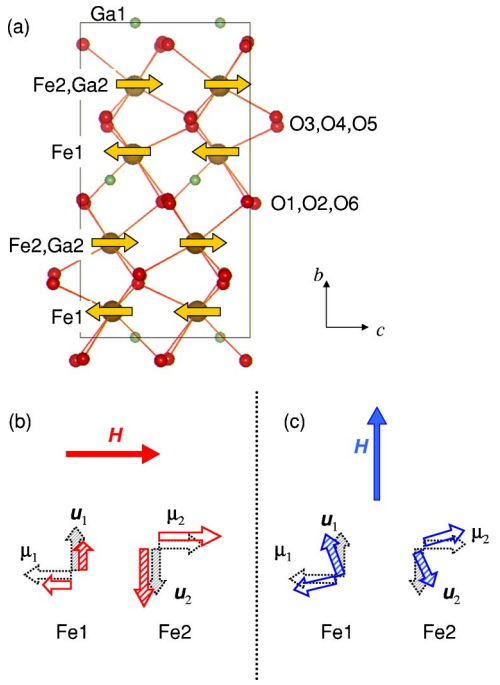

FIG. 4. (Color online) (a) Magnetic structure of $GaFeO_3$. Arrows indicate Fe moments. Note that the positions of Fe1 and Fe2 are shifted to $+b$ and $-b$, respectively, from the center of the two adjacent oxygen layers. (b), (c) Qualitative explanation of a large difference between the α_{bc} and α_{cb} values. Local displacement $\boldsymbol{u_i}$ from the center of the octahedron and magnetic moment $\boldsymbol{\mu_i}$ on Fei site ($i=1,2$) in zero (thin dotted lines; black in online version) and strong (thick lines; red and blue in online version) magnetic fields $\boldsymbol{H}$. The modulations of $\boldsymbol{u}_1$ and $\boldsymbol{u}_2$ are cooperative in the case of $H\|c$ as shown in (b), whereas they tend to cancel out in the case of $H\|b$ (c).

canted ferromagnetic structure. The obtained magnetic structure is displayed in Fig. 4(a). Rietveld analysis of a TOF diffraction pattern at 4 K indicates that the magnetic moment of high-spin Fe^{3+} on a Ga2 site is aligned parallel with Fe2. The obtained parameters of the Fe^{3+} magnetic moments on the Fe1, Fe2, and Ga2 sites are -3.9, $+4.5$, and $+4.7$ μ_B per Fe ion, respectively. (The Fe moment on a Ga1 site could not be determined because the Fe occupancy is too small.) Since the sum of Fe amount at the Fe2 and Ga2 sites is larger than the Fe amount on Fe1, antiferromagnetic alignment of the Fe moments causes the ferrimagnetic magnetization along the c axis.

From a crystallographic point of view, the displacement of an Fe ion from the center of the oxygen octahedron along the b axis as well as the spin moment along the c axis is arranged in opposite directions for Fe1 and Fe2 as indicated by Fig. 4(a). Consequently, the outer products of displacement and magnetic-moment vectors at Fe1 and Fe2 are in the same direction, which would be one of the possible origins of the large ME effect in $GaFeO_3$, as Popov *et al.* have previously pointed out.[16] This situation is rather similar with a typical antiferromagnetic ME material Cr_2O_3. In Cr_2O_3, Cr ions on two magnetic sublattices shift along c by about 0.23 Å in the opposite direction to each other.

TABLE III. Lattice parameters with the $Pc2_1n$ setting and Ga/Fe partial occupancies at the Ga1, Ga2, Fe1, and Fe2 sites [see Figs. 1(a) and 1(b)] as deduced by a Rietveld analysis of synchrotron x-ray diffraction at room temperature.

x	0.80	1.00	1.20
a	8.7358(13)	8.7442(10)	8.7515(15)
b	9.3771(14)	9.3927(11)	9.4012(16)
c	5.0767(7)	5.0823(5)	5.0865(9)
Ga1	0.93/0.07	0.90/0.10	0.74/0.25
Ga2	0.80/0.20	0.76/0.24	0.55/0.45
Fe1	0.35/0.65	0.16/0.84	0.14/0.86
Fe2	0.32/0.68	0.17/0.83	0.15/0.85

V. SYNCHROTRON X-RAY DIFFRACTION

Synchrotron x-ray powder diffraction patterns of $Ga_{2-x}Fe_xO_3$ ($x=0.8, 1.0$, and 1.2) were measured at Photon Factory Beam-line 1A, KEK, Japan. The x-ray wavelength was 0.689 Å and the diffraction at room temperature was detected by a curved imaging plate. The change in lattice parameters and occupation at the crystallographically inequivalent four cation sites with the Fe content x was examined by Rietveld analysis with RIETAN-2000.[22] The obtained patterns were well reproduced by a $Pc2_1n$ orthorhombic cell. The results were summarized in Table III. The nearly isotropic change in the lattice parameters with the composition is mostly due to the difference in ionic radius between Fe and Ga.

The absolute values of occupation are not accurate because of the small difference in x-ray atomic scattering factor between Fe^{3+} and Ga^{3+}. The ratio of x-ray atomic scattering factors in two ions is smaller, even in the case of $2\theta=0$, than the ratio of the neutron scattering section of Fe (9.45) to that of Ga (7.29). The difference of the x-ray scattering factor becomes smaller as the scattering angle 2θ increases, while the neutron scattering section depends little on 2θ. The standard deviations of the occupations obtained from the analysis of x-ray diffraction are 0.02–0.05. However, the tendency of the change in Ga/Fe occupancy with x may be acceptable and qualitatively agrees with the neutron data. Most excess Fe ions in $x>1.0$ compounds are likely to replace Ga at the octahedral Ga2 sites. Fairly strong antiferromagnetic superexchange interaction between neighboring Fe^{3+} ions at the Fe1 and Ga2 sites possibly reinforces the ferrimagnetic spin ordering. The occupation of Ga at the Fe1 and Fe2 sites becomes less with increasing the Fe content x, which should also stabilize the ferrimagnetic state.

VI. MAGNETOELECTRIC (ME_H) EFFECTS

ME_H effects in $Ga_{2-x}Fe_xO_3$ were measured by sweeping an external magnetic field at a constant rate (the so-called DC_H method). Three plate-shaped samples were prepared for each composition x. The typical dimension was 25 mm^2 in area and 1 mm in thickness. The three have the (100), (010),

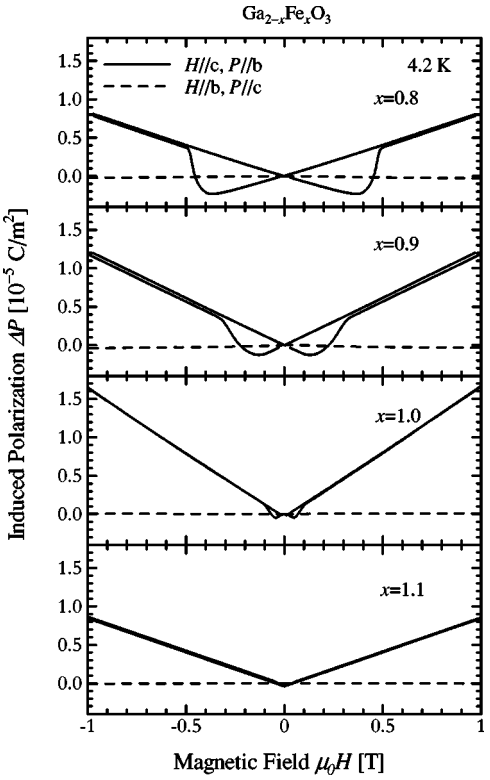

FIG. 5. Dependence of magnetoelectric polarization on magnetic field, ΔP_b versus H_c (solid lines) and ΔP_c versus H_b (dashed lines). Measurements were performed for the crystals immersed in liquid helium, i.e., at 4.2 K. Before a measurement of α_{cb}, a high magnetic field was applied along the *c* axis at 4.2 K to make the magnetization saturated.

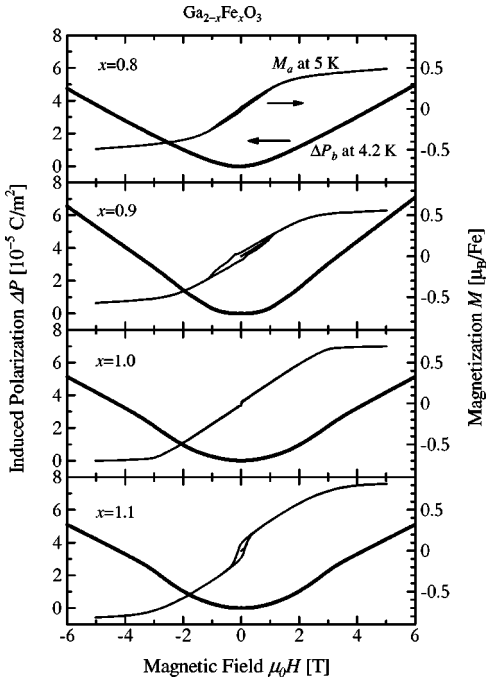

FIG. 6. Thick lines: magnetoelectric polarization (ΔP_b) as a function of a magnetic field (H) applied parallel to the *a* axis. Measurements were performed for the crystals immersed in liquid helium, i.e., at 4.2 K. Thin lines: magnetization at 5 K with $H \| a$.

and (001) surfaces, respectively. Ag electrode was deposited onto the both end surfaces of each sample and heated at 400 °C to form an electric capacitor. The capacitor was cooled in a cryostat with a superconducting magnet (Oxford SM4000). Prior to each measurement of α_{cb}, the sample was cooled in a stronger magnetic field than 0.15 T to align the magnetization direction. Electric current induced by sweeping a magnetic field with a constant rate of 7.6 mT/s was monitored by an electrometer (Keithley 6517A). Induced polarization (ΔP) was calculated by integration of the induced current. All the measurements of a ME_H effect were performed with the respective sample immersed in liquid He.

Considering the $Pc'2'_1n$ magnetic space group of $Ga_{2-x}Fe_xO_3$, two components of linear ME tensor, α_{bc} and α_{cb}, are expected to be nonzero. The butterfly-shape behavior[23] was clearly observed in all the $\Delta P_b - H_c$ curves as shown in Fig. 5, while little polarization along the *c* axis was induced by application of a magnetic field along the *b* axis. In higher magnetic fields along the *c* axis than the coercive force, the induced polarization along *b* is linearly dependent on H. The value of α_{bc} was obtained from the linear part of a $\Delta P_c - H_c$ curve in each panel of Fig. 5. The observed butterfly curves are ascribed to the magnetization reversal process. The field where the polarization abruptly increases corresponds well to the coercive force in each magnetization curve at 5 K displayed in Fig. 2. In both measurements of magnetization and ME_H, it is clearly shown that the coercive force declines with the increase of the iron content x. As x increases, more Fe ions occupy Ga1 or Ga2 sites. The $3d$ electron distribution in a $3d^5$ Fe^{3+} ion at a less distorted oc-

TABLE IV. Linear and quadratic magnetoelectric coefficients α_{ij} and β_{bii} at 4.2 K as obtained from the so-called DC_H method for floating-zone grown single crystals of $Ga_{2-x}Fe_xO_3$. (See text for the definition of α_{ij} and β_{bii}.)

x	α_{bc} (10^{-11} s/m)	α_{cb} (10^{-11} s/m)	β_{baa} (10^{-15} s/A)	α_{ba} (10^{-11} s/m)[a]	β_{bbb} (10^{-15} s/A)
0.8	1.26(20)	<0.1	9.34	1.05(20)	3.81
0.9	1.80(20)	<0.1	12.23	1.26(20)	1.99
1.0	2.10(20)	<0.1	7.69	1.01(20)	2.85
1.1	1.05(20)	<0.1	8.03	1.05(20)	5.98

[a]These values apply only in magnetic fields high enough to make the magnetization along the *a* axis saturated.

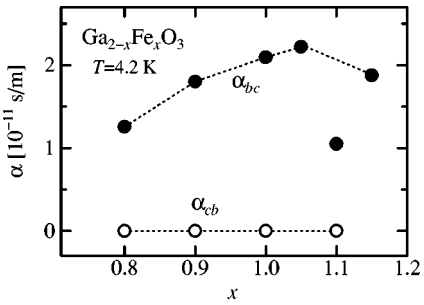

FIG. 7. Linear magnetoelectric coefficients α_{bc} (solid circles) and α_{cb} (open circles) as functions of x for floating-zone grown single crystals of $Ga_{2-x}Fe_xO_3$. Dotted lines are merely the guide to the eyes.

tahedral Ga2 site is perhaps less anisotropic, which should reduce magnetic anisotropy of the compound. There is also a possibility that the partial occupation of Fe on the Ga1 sites would affect the magnetic anisotropy of the compound.

In a magnetic field parallel to the b axis, electric polarization along the c axis was hardly induced as shown by broken lines in Fig. 5. The value of α_{cb} for every composition x is calculated to be less than 10^{-12} s/m. The sharp contrast between the α_{bc} and α_{cb} values can be qualitatively understood as follows [see Fig. 4(b)]. In the $H\|c$ case where a magnetic field is parallel to the Fe spin moments, the Fe2 moment increases while Fe1 moment decreases. (Here the moment stands for that in both spin and orbital sectors.) If the displacement along the b axis of Fe2 is enlarged by the modulation of the magnetic moment, that of Fe1 is reduced, conversely. Since the displacements of Fe1 and Fe2 are opposite in direction with each other, the magnetic-field-induced modulation of the displacement cooperatively affects the bulk polarization P_b as a result. In the $H\|b$ case, a magnetic field makes the Fe2 moment canted toward the $+b$ direction, when the Fe1 moment is canted toward the $-b$ direction. Here one should note that the energy scale of magnetic fields used in the present study was much weaker than the exchange interaction J between neighboring Fe ions. If Fe2 would be shifted to the $+c$ direction by the rotation of the spin moment, the shift of Fe1 would be directed to the $-c$ direction. The shifts of Fe1 and Fe2 along the c axis should be opposite in direction and hence partially cancelled out in terms of the bulk polarization.

The *linear* ME_H effect should not be observed in any configuration other than P_bH_c and P_cH_b according to the magnetic space group. However, the polarization along the b axis (P_b) is also modulated by applying a magnetic field along either the a or b axis. The polarization along the b axis induced by the application of a magnetic field along the a axis is displayed in comparison with the magnetization curve in the $H\|a$ configuration in Fig. 6. In low magnetic fields, the magnetic-field-induced polarization along the b axis was fitted with a quadratic function of magnetic field, $\Delta P_b = \frac{1}{2}\beta_{baa}H_a^2$. This is consistent with the absence of the linear ME coefficient α_{ba} in the $Pc'2_1'n$ space group. With increasing a magnetic field, the magnetization along the direction becomes saturated as shown by thin lines. In high magnetic fields where the magnetization is saturated, the induced polarization is dependent not quadratically but linearly on a field. In such a high field, it is convenient to discuss in terms of a magnetic point group $m2'm'$. Nonzero components of the linear ME tensor in the symmetry are α_{ab} and α_{ba}. The latter can explain the high-field behavior of the $\Delta P_b - H_a$ curve. In the $P_b - H_b$ configuration, a similar quadratic-linear crossover behavior of magnetic-field-induced polarization would be expected. However, the magnetic field used in this study was not high enough to make the magnetization along the b axis saturated, because it is the hard axis as shown in Fig. 2. We hence analyzed the low-field curve using only the quadratic ME component β_{bbb}.

Linear and quadratic ME coefficients in FZ crystals of $Ga_{2-x}Fe_xO_3$ obtained in this study are summarized in Table IV. The β_{baa} values are larger than the β_{bbb} values, which may be partly due to the anisotropic magnetic susceptibility. Figure 7 shows x dependence of linear ME coefficients. As discussed above, the large ME coefficient α_{bc} can be ascribed to Fe^{3+} ions at Fe1 and Fe2. The total amount of Fe^{3+} ions at Fe1 and Fe2 increases with increasing Fe content x as shown in Tables II and III. The overall feature of the x-dependence of α_{bc} shown in Fig. 7 can be explained by the change in Fe occupancies at Fe1 and Fe2. The anomalously small α_{bc} for the $x=1.10$ sample may be possibly due to the twinned structure in polarization direction.

VII. SUMMARY

We have succeeded in growing large single crystals of a series of polar ferrimagnetic compounds $Ga_{2-x}Fe_xO_3$ ($0.8 \leqslant x \leqslant 1.4$) by a FZ method under a high oxygen pressure of 9–10 atm. With the increase of Fe content x, the Curie temperature and the saturated magnetization increase, while the coercive force decreases. A neutron diffraction study suggested that the basic crystal structure is almost the same as the flux-grown crystal, although the Curie temperature of the FZ-melt crystal is considerably lower than the flux crystal with the same composition. The lower T_C of the melt-grown crystal should be ascribed to the higher Fe occupation at the Ga1 sites, which would be specific to the high-temperature synthesis.

The magnetic point group is $m'2'm$, which is consistent with the previous studies. Two components α_{bc} and α_{cb} of the linear ME tensor were predicted to be finite from the group theory. The α_{bc} value was obtained to be $1\sim2 \times 10^{-11}$ s/m from a DC_H method, which is as large as that reported on the flux-grown crystal in literature. In contrast, the electric polarization along the c axis induced by a magnetic field parallel to the b axis was not detected in the present study. A possible microscopic origin of the sharp contrast in the linear ME effects between the two configurations was proposed.

ACKNOWLEDGMENTS

The authors are grateful to Professor K. Kohn for fruitful discussions. This work was partly supported by Ministry of Education, Culture, Sports, Science and Technology, Japan.

*Corresponding author; present address: Institute of Multidisciplinary Research for Advanced Materials, Tohoku University, Sendai 980-8577, Japan; electronic address: arima@tagen.tohoku.ac.jp

†Present address: Los Alamos National Laboratory, Los Alamos, NM 87545.

[1] J. P. Remeika, J. Appl. Phys. **31**, 263S (1960).

[2] E. A. Wood, Acta Crystallogr. **13**, 682 (1960).

[3] S. C. Abrahams, J. M. Reddy, and J. L. Bernstein, J. Chem. Phys. **42**, 3957 (1965).

[4] E. F. Bertaut, G. Bassi, G. Buisson, J. Chappert, A. Delapalme, R. Pauthenet, H. P. Rebouillat, and R. Aleonard, J. Phys. (Paris) **27**, 433 (1966).

[5] A. Delapalme, J. Phys. Chem. Solids **28**, 1451 (1967).

[6] We describe the space group of the compound as $Pc2_1n$, which has been used in previous articles, to avoid confusion, though the notation of $Pna2_1$ is recommended in the international table.

[7] R. B. Frankel, N. A. Blum, S. Foner, A. J. Freeman, and M. Schieber, Phys. Rev. Lett. **15**, 958 (1965).

[8] J.-P. Rivera, Ferroelectrics **161**, 165 (1994). Note that $J=\mu_0 M$ was used as the definition of magnetization in the reference.

[9] G. T. Rado, Phys. Rev. Lett. **13**, 335 (1964).

[10] R. V. Pisarev, Zh. Eksp. Teor. Fiz. **58**, 1421 (1970) [Sov. Phys. JETP **31**, 761 (1970)].

[11] For a review, K. H. Bennemann, *Nonlinear Optics in Metals* (Clarendon Press, Oxford, 1998).

[12] M. Fiebig, D. Fröhlich, B. B. Krichevtsov, and R. V. Pisarev, Phys. Rev. Lett. **73**, 2127 (1994); D. Fröhlich, S. Leute, V. V. Pavlov, and R. V. Pisarev, *ibid.* **81**, 3239 (1998).

[13] Y. Ogawa, Y. Kaneko, J. P. He, X. Z. Yu, T. Arima, and Y. Tokura, Phys. Rev. Lett. **92**, 047401 (2004).

[14] M. Kubota, T. Arima, J. P. He, Y. Kaneko, J. P. He, X. Z. Yu, and Y. Tokura, Phys. Rev. Lett. **92**, 137401 (2004).

[15] J. H. Jung, M. Matsubara, T. Arima, J. P. He, Y. Kaneko, and Y. Tokura, Phys. Rev. Lett. **93**, 037403 (2004).

[16] Yu. F. Popov, A. M. Kadomtseva, G. P. Vorob'ev, V. A. Timofeeva, D. M. Ustinin, A. K. Zvezdin, and M. M. Tegeranchi, Zh. Eksp. Teor. Fiz. **114** 263 (1998) [JETP **87**, 146 (1998)].

[17] H. J. Van Hook, J. Am. Ceram. Soc. **48**, 471 (1965).

[18] C. H. Nowlin and R. V. Jones, J. Appl. Phys. **34**, 1262 (1963).

[19] A. Pinto, J. Appl. Phys. **37**, 4372 (1966).

[20] J. H. Schelleng and G. T. Rado, Phys. Rev. **179**, 541 (1969).

[21] T. Ohta, F. Izumi, K. Oikawa, and T. Kamiyama, Physica B **234-236**, 1093 (1997).

[22] F. Izumi and T. Ikeda, Mater. Sci. Forum **321-324**, 198 (2000).

[23] E. Ascher, H. Rieder, H. Schmid, and H. Stössel, J. Appl. Phys. **37**, 1404 (1966).